Laser Physics, Vol. 11, No. 2, 2001, pp. 269–277.

Rare Gas Cluster Explosion in a Strong Laser Field

K. Ishikawa and T. Blenski

CEA-Saclay, DSM/DRECAM/SPAM, Bât. 522, Gif-sur-Yvette Cedex, 91191 France

e-mail: ishikawa@cea.fr

Received August 12, 2000

Abstract—We study the ionization and explosion dynamics of rare gas clusters containing up to 147 atoms in an intense, femtosecond laser pulse via Monte Carlo particle dynamics simulations. Our method includes tunnel and impact ionization as well as ion–electron recombination, and allows us to follow the motion of both ions and free electrons during laser–cluster interaction. The simulation results show that ionization proceeds mainly through tunnel ionization by the combined fields from ions, electrons and laser while the contribution of electron impact ionization is secondary. Concerning explosion dynamics, the ions are ejected in a stepwise manner from outer shells and accelerated mainly through their mutual Coulomb repulsion. If we take a spatial laser intensity profile into account properly, this Coulomb explosion leads to the same charge dependence of ion energy, i.e., quadratic for lower charge states and linear for higher ones, as that observed in experiments with larger clusters. This indicates that Coulomb explosion may be a dominant cluster explosion mechanism even in the case of large clusters.

1. INTRODUCTION

Since the advent of high-intensity ($>10^{14}$ W/cm^2), short-pulse (<1 ps) lasers, their interaction with rare gas clusters has been extensively studied [1–11]. Although the global density of a cluster gas may be arbitrarily low, its high local density leads to strong absorption of laser energy. The experimental observation of highly charged ions [1, 2], high ion kinetic energy [3], high electron temperature [4], and X-ray emission in the keV range [5] has revealed surprisingly high energetic nature of the interaction.

Theoretical modeling of the intense laser pulse interaction with rare gas clusters is a challenging subject involving the nonlinear, nonperturbative response of many ions and electrons. The laser–cluster interaction involves two processes, i.e., ionization and explosion. Several models have been developed on the ionization mechanism which leads to the production of unusually high charge states. In a coherent electron motion model by McPherson *et al.* [6], multiple ionization arises from impact by coherently moving electrons, behaving like a quasi-particle. Ditmire *et al.* [7, 8] proposed a "nanoplasma" model, in which ions are ionized mainly through impact of hot electrons heated by inverse bremsstrahlung. Rose-Petruck *et al.* [9] introduced an "ionization ignition (II)" model, where ionization is driven by the combined field of the laser, the other ions, and the electrons. Concerning the explosion dynamics, related to the high ion energy, the nanoplasma model [7, 8] suggests that the cluster expands in a hydrodynamic manner by the pressure of hot electrons confined inside the cluster by space charge effect. However, Last and Jortner [10, 11], who performed classical dynamics simulations using the approximation of frozen ion positions, fixed number of free electrons, and smoothed ion–electron and electron–electron interaction, showed that electrons relatively quickly leave even large xenon clusters containing over 2000 atoms and, therefore, that the existence of the nanoplasma confined inside the cluster is questionable.

In the present study, we improve the Monte Carlo particle dynamics simulation presented in [8], and investigate the ionization and explosion dynamics of rare gas clusters (Ar_{55}, Ar_{147}, Xe_{55}, and Xe_{147}) irradiated by a ultrashort intense laser pulse using this method. In Section 2 we briefly summarize our simulation method. The equations of motion of the ions and the free electrons are numerically integrated with the force calculated as the sum of the contributions from the laser field and real (singular) Coulomb potentials of the other particles. Free electrons may appear through tunneling ionization and electron impact ionization, and may recombine with ions. This method allows us to follow the motion of both ions and free electrons during the cluster explosion. In Section 3, we discuss the importance of tunnel and electron impact ionization in laser–cluster interaction. Our results indicate that the former is the dominant ionization mechanism and that the latter plays only a minor role. In Section 4, we examine the mechanism of cluster explosion with special focus on the charge dependence of ion energy. Experimental work by Lezius *et al.* [2] has shown that the dependence is quadratic in the case of Ar while it is quadratic at lower charge states and linear at higher charge states in the case of Xe. In [2] the quadratic dependence was attributed to Coulomb explosion, and the linear one to hydrodynamic expansion. However, the analysis of our simulation results, which lead to a similar behavior, shows that this charge-energy relation can be entirely explained on the basis of the Coulomb explosion mechanism if we take a spatial laser intensity profile into account properly. The conclusions are given in Section 5.

2. SIMULATION METHOD

A basic idea of our simulation method is to treat ions and free electrons as classical point particles and to integrate the nonrelativistic equations of motion for them. Bound electrons do not appear explicitly. This idea is based on the fact that the essence of many phenomena involving an intense laser field such as above threshold ionization [12] and high-order harmonic generation [13] can be well described by treating the ejected electron as a classical particle without taking account of the response of bound electrons. The force acting on each particle is calculated as the sum of the contributions from all the other particles and the laser electric field. To account for the finite size of the electron cloud around each nucleus, the field from an ion of charge state Q is modeled as a Coulomb one from an effective nuclear charge $Q_{\rm eff}(r)$ of the form,

$$Q_{\rm eff}(r) = \begin{cases} Z(1-r/r_a) & \text{for} \quad r < (Z-Q)r_a/Z, \\ Q & \text{for} \quad r \geq (Z-Q)r_a/Z, \end{cases} \tag{1}$$

with Z being the atomic number and r_a, the "atomic radius," calculated using self-consistent-field functions [14], which takes the value of 1.3 a.u. for Ar and 2.0 a.u. for Xe. We use atomic units throughout this paper unless otherwise stated. $Q_{\rm eff}(r)$ tends to the bare nuclear charge Z as r tends to zero. This potential is more suitable for the description of ion–electron interaction, which may lead to the confinement of electrons inside the cluster and inverse bremsstrahlung, than a soft Coulomb potential used by Ditmire [8]. The equation of motion of particles are integrated with the fifth order Cash–Karp Runge–Kutta method with adaptive stepsize control [15]. In a situation where an electron happens to be very close to an ion, the use of a real Coulomb potential might lead to serious problems, i.e., very small time steps and numerical heating. To circumvent these problems, we resort to Kustaanheimo–Stiefel regularization [16–18], widely used in astrophysical simulations. This is an efficient method to transform the equations of the relative two-body motion into a form that is well behaved for small separations.

In an intense laser field, the cluster atoms may be ionized by tunnel ionization (optical field ionization). We evaluate the probability of ionization per unit time $W_{\rm tun}$ from a state with orbital number l of an ion with charge Q via the following analytic formula [19, 20],

$$W_{\rm tun} = \sum_{m=-l}^{l} \frac{(l+|m|)!}{2^{|m|}|m|!(l-|m|)!}\left(\frac{2e}{n^*}\right)^{2n^*}\frac{I_p}{2\pi n^*} \times\left(\frac{2(2I_p)^{3/2}}{E}\right)^{2n^*-|m|-2}\exp\left(-\frac{2(2I_p)^{3/2}}{3E}\right), \tag{2}$$

where I_p denotes the ionization potential, E the total electric field seen by the ion, and n^* the effective principal quantum number defined by,

$$n^* = (Q+1)[2I_p]^{-1/2}. \tag{3}$$

The rate $W_{\rm tun}$ in Eq. (2) is averaged over the magnetic quantum number m. If a random number $p \in [0, 1]$ is smaller than the tunneling probability $W_{\rm tun}\Delta t$ during a time step Δt, the tunnel ionization occurs. Then a new electron is placed with zero velocity near the parent ion in the direction of the ionizing field in such a way that the total energy of the system is conserved. Depending on the positions of the ions and the other electrons, there happens to be situations where it is impossible to put a new electron into the simulated system, guaranteeing the energy conservation at the same time. In such cases, ionization is cancelled.

Free electrons may appear also through electron impact ionization (collisional ionization). An electron impact ionization occurs if the distance between an electron and an ion is decreasing and if the impact parameter b and the electron impact ionization cross section $\sigma_{\rm EII}$ satisfy the relation

$$4\pi r_0|r_0 - b| < \sigma_{\rm EII}, \tag{4}$$

where r_0 is obtained from

$$U_{Q+1}(r_0) = I_p, \tag{5}$$

with $U_Q(r)$ being the potential of an ion with a charge of Q. We calculate $\sigma_{\rm EII}$ using fitting formulas by Lennon *et al.* [21] for Ar and the Lotz formula [22],

$$\sigma_{\rm EII} = aq\frac{\ln(E_e/I_p)}{E_e I_p} \quad (E_e > i_p), \tag{6}$$

for Xe, where $a = 4.5 \times 10^{-14}$ (cm^2 eV^2), q is the number of electrons in the outer shell of the ion, and E_e is the energy of the impact electron. Upon ionization a new electron is placed at the distance r_0 from the ion with the position and velocity chosen randomly with a condition that the total energy and momentum are conserved.

In the laser–cluster interaction free electrons may be recombined with ions. A pair of an ion with a charge Q and an electron is replaced by an ion with a charge $Q-1$ if the distance between them is decreasing, if there is no potential barrier between them, and if the following relation is satisfied:

$$\sum_j (Q_j/|\mathbf{X}-\mathbf{X}_j| - U_{Q_j}(|\mathbf{x}-\mathbf{X}_j|)) - \sum_i\left(U_Q(|\mathbf{X}-\mathbf{x}_i|) - U_{Q-1}(|\mathbf{X}-\mathbf{x}_i|) - \frac{1}{|\mathbf{x}-\mathbf{x}_i|}\right) - U_Q(|\mathbf{x}-\mathbf{X}|) + \mathbf{F}_L\cdot(\mathbf{x}-\mathbf{X}) + \frac{v^2}{2} < 0, \tag{7}$$

where $\mathbf{x}$ is the electron position, $\mathbf{X}$ the ion position, $\mathbf{F}_L$ the laser field, and v the electron velocity. The first sum is taken over all the other ions j of a position $\mathbf{X}_j$ and a charge Q_j, and the second sum over all the other electrons i of a position $\mathbf{x}_i$. If there were no other ions or electrons than the ion–electron pair, the inequality Eq. (7) would be reduced to the following expression:

$$-U_Q(|\mathbf{x}-\mathbf{X}|)+\mathbf{F}_L\cdot(\mathbf{x}-\mathbf{X})+\frac{v^2}{2}<0, \qquad (8)$$

which states that the total energy of the electron is negative. The first two terms of Eq. (7) are the correction due to the presence of the other ions and electrons.

It is true that our simple way to implement recombination would not reproduce its rate accurately, but our goal is not to develop a highly sophisticated semiclassical model, but to mimic correctly the explosion dynamics of clusters. Moreover, the inclusion of recombination has the following advantage. A problem which may be encountered in classical particle simulations using a singular Coulomb potential is that some electrons can gain high energy and escape the cluster while others lose much energy. This unphysical process is suppressed thanks to the inclusion of recombination, which prevents the formation of tightly bound ion–electron systems.

The pulse used in the simulations has a field envelope proportional to sine squared with a full width at half maximum of 100 fs and a wavelength of 780 nm. The initial geometry of the clusters is chosen to be a closed shell icosahedral structure [23] with an atom spacing of 3.7 Å for Ar and 4.4 Å for Xe [24]. The shell structure of Ar and Xe clusters is summarized in the table.

3. IONIZATION MECHANISM

Figure 1 shows the temporal evolution of the mean ion charge state obtained from an Ar_{147} cluster (solid line) and individual Ar atoms (dashed line) irradiated by a laser pulse with a peak intensity of 1.4×10^{15} W/cm^2. The mean charge state obtained in a cluster gas is considerably higher than that in an atomic gas. Moreover, in our simulations highly charged ions up to Ar^{8+} were obtained from the cluster gas though it is not explicitly indicated in the figure.

Our simulation method includes two possible ionization processes: tunnel and electron impact ionization. According to the nanoplasma model [7, 8], the principal ionization mechanism is electron impact ionization by hot electrons heated through inverse bremsstrahlung. On the other hand, the ionization ignition model [9] indicates that tunnel ionization by the combined field of the laser, the other ions, and the electrons plays a dominant role. Strictly speaking, the distinction between tunnel ionization by an electronic field and electron impact ionization is not unambiguous,

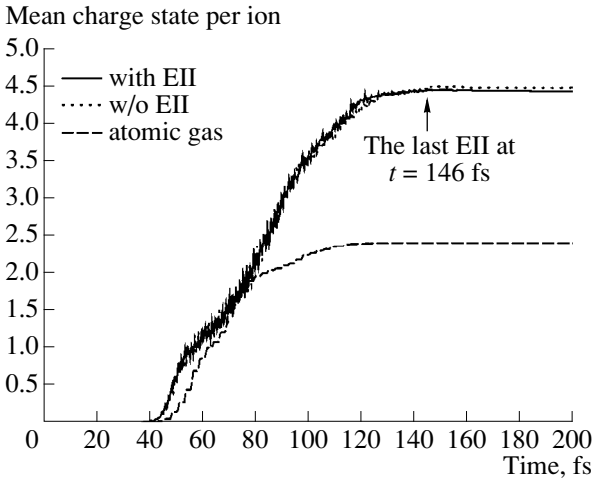

Fig. 1. Evolution of the mean charge state per ion in Ar_{147} (solid line) and an atomic gas of Ar (dashed line) irradiated by the pulse with a peak intensity of 1.4×10^{15} W/cm^2. The dotted line is the result for Ar_{147} with electron impact ionization switched off.

since the latter is also due to the field of an incident electron. Nevertheless, in the present study, let us refer to the ejection of a bound electron by an incident energetic electron as electron impact ionization and distinguish it from tunnel ionization due to the field formed by many electrons. Multiple ionization from impact by coherently moving electrons proposed in the coherent electron motion model [6] would be, if any, a purely quantum mechanical effect, and, therefore, is outside the scope of the present study.

In order to examine the effect of electron impact ionization on the mean charge state, we have performed a simulation with electron impact ionization switched off, whose result is shown as a dotted line in Fig. 1. It can be seen that electron impact ionization has practically no effect on the mean charge. Moreover the highest charge state produced by electron impact ionization was 5+. This result can be easily understood from the

Shell structure of Ar and Xe clusters. Each shell forms an icosahedron. Shells II and III contain two and three subshells, respectively

Shell	Subshell	Number of atoms	Distance from the center (Å)	
			Ar	Xe
Central atom		1	0	0
I	1	12	3.7	4.4
II	2	30	6.3	7.5
	3	12	7.4	8.8
III	4	20	8.9	10.5
	5	60	9.7	11.4
	6	12	11.2	13.2

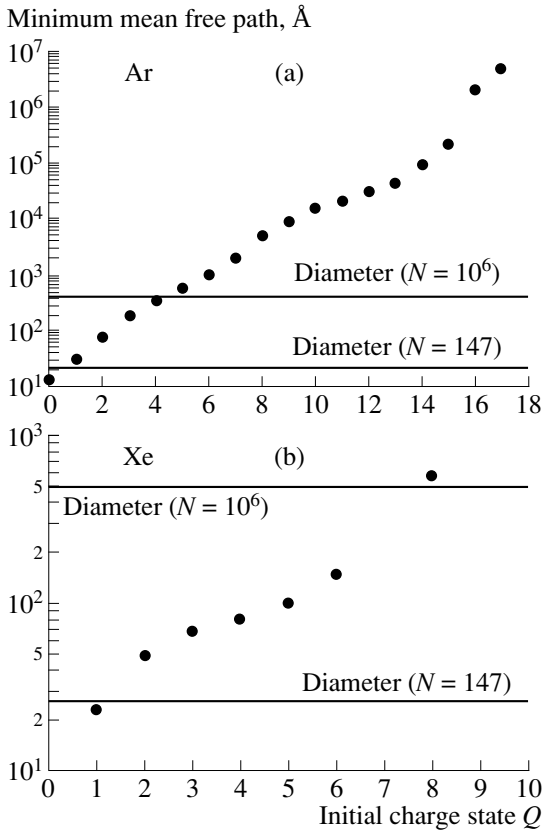

Fig. 2. (a) Minimum electron mean free path inside the Ar cluster with respect to electron impact ionization $Ar^{Q+} \longrightarrow Ar^{(Q+1)+}$ ($0 \le Q \le 17$) calculated for the incident electron energy at which the cross section σ_{EII} takes a maximum value. The diameter of an Ar_{147} and Ar_{10^6} is also indicated. (b) Similar plot for the case of the Xe cluster ($Q = 1, \ldots, 6, 8$).

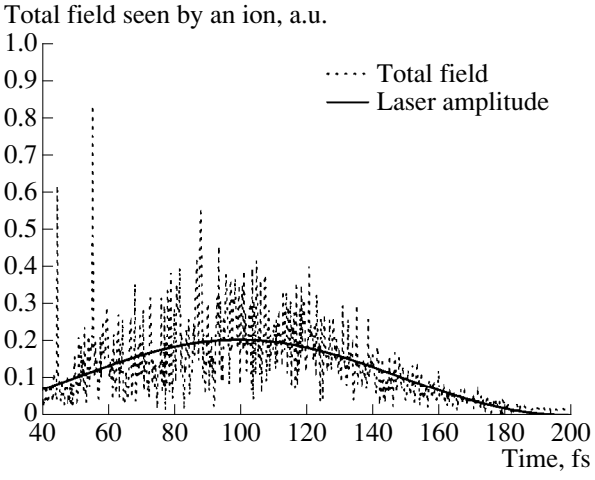

Fig. 3. Evolution of the total electric field strength (dashed line) seen by an Ar ion of the outermost subshell of Ar_{147} and that of the amplitude of the laser field alone (solid line) for the case of Fig. 1.

viewpoint of the mean free path of electrons inside the cluster. The mean free path λ_{EII} with respect to electron impact ionization is defined by $\lambda_{EII} = 1/N_a\sigma_{EII}(E_e)$, where N_a is the atomic density inside the cluster. λ_{EII} takes the minimum value at a certain value of incident electron energy E_e (minimum mean free path). We show the minimum mean free path as a function of initial ion charge Q for Ar and Xe clusters in Fig. 2. In this figure we also indicate the diameter of the cluster containing 147 and 10^6 atoms. As can be seen from Fig. 2, the minimum mean free path exceeds the size of Ar_{147} already at $Q = 1$ and that of Xe_{147} at $Q = 2$. Moreover, for $Q \ge 5$ in the case of Ar and $Q \ge 8$ in the case of Xe, the minimum mean free path is larger than the size of a cluster containing 10^6 atoms. It should be noted that in general the electron mean free path is larger than the minimum value plotted in Fig. 2. Hence, electron impact plays only a minor role in ionization even in the case of very large clusters.

In Fig. 3 we show the temporal evolution of the total electric field seen by an ion, together with the amplitude of the laser field, for the case of Fig. 1. As can be seen from Fig. 3, once several atoms are ionized, the total electric field strength at the position of each cluster ion can be significantly larger than the laser field alone. This drives further tunneling ionization and leads to high charge states just as was proposed in the ionization ignition model [9].

At a glance, our results may appear to contradict those in [8] obtained using a simulation method similar to ours. Figure 2b of [8] shows, however, that the level of ionization is larger when impact ionization *and* electron fields in tunnel ionization are included than when they are neglected. The effect of impact ionization *alone* was not examined in [8]. On the other hand, the present study clearly shows that electron impact plays a negligible role in ionization.

4. EXPLOSION MECHANISM

We can consider two different explosion mechanisms of clusters irradiated by an ultrashort intense laser pulse: Coulomb explosion and hydrodynamic expansion. Coulomb explosion is expected to be a dominant mechanism in case where ejected electrons escape from the cluster quickly. In this case the accumulated total Coulomb energy is converted into ion kinetic energy. Thus, we can approximate the relation between the mean ion energy $\bar{E} = \sum_{j=1}^{N} E_j/N$ and the mean ion charge state $\bar{Q} = \sum_{j=1}^{N} Q_j/N$, with E_j and Q_j being the kinetic energy and the charge state, respectively, of ion j, and N the number of atoms contained in the cluster, as

$$\bar{E} = \frac{\bar{Q}^2}{N} \sum_{i=1}^{N-1} \sum_{j=i+1}^{N} \frac{1}{|\mathbf{R}_i - \mathbf{R}_j|} \propto \bar{Q}^2, \qquad (9)$$

where $\mathbf{R}_i$ denotes the initial position of ion i. On the other hand one expects that the cluster explodes mainly through hydrodynamic expansion in case where most of free electrons are confined inside the cluster by space-charge effect for a long time. In this case, the thermal energy of hot electrons is transformed into ion kinetic energy. Then, the relation between the mean energy and mean charge of the ions is approximately given by

$$\bar{E} = \frac{3}{2}\bar{Q}k_B T_e \propto \bar{Q}, \qquad (10)$$

where k_B is Boltzmann constant, and T_e the electron temperature. This relation is linear under the assumption that T_e does not depend much on $\bar{Q}$.

Lezius *et al.* [2] obtained experimentally the charge dependence of the kinetic energy of the ions emitted from laser-irradiated Ar and Xe clusters. This dependence was used to determine when the cluster explosion is governed by Coulomb explosion and when by hydrodynamic expansion. Their results can be summarized as follows: in the case of Ar, the charge dependence of the ion energy is quadratic in the entire range of $1 \le Q \le 8$, while in the case of Xe, the dependence is quadratic for lower charge states ($Q < 6$) and linear for higher charge states ($Q > 10$).

Based on these results and the discussion in the preceding paragraph, the authors of [2] have concluded that Ar clusters undergo Coulomb explosion while Xe clusters exhibit a mixed Coulomb-hydrodynamic expansion behavior. Equations (9) and (10) describe, however, the relation between the *mean* energy and the *mean* charge state of the ions, and do not necessarily hold true for the charge-energy relation of *individual* ions, obtained in the experiments by Lezius *et al.* [2]. In what follows, we examine the charge-energy relation obtained from our simulation results in detail.

In Fig. 4 we plot the relation between the mean ion energy $\bar{E}$ and mean charge state $\bar{Q}$ obtained using different laser intensities for Ar_{55}, Ar_{147}, Xe_{55}, and Xe_{147}. The relation can be modeled with $\bar{E} \approx \alpha \bar{Q}^2$, where α is a constant. This indicates that ions are accelerated mainly through a Coulomb explosion mechanism. The value of α indicated in Fig. 4 is smaller than the one (57, 115, 41, and 75 eV for Ar_{55}, Ar_{147}, Xe_{55}, and Xe_{147}, respectively) which can be calculated from Eq. (9). This is because the charge state of each ion changes in time, and because the cluster explosion begins before the ion charges reach their final values.

In Fig. 5a we show the temporal evolution of the total number of free electrons and the number of free electrons inside the cluster for the case of a Xe_{147} cluster irradiated by a laser pulse with a peak intensity of 8.8×10^{15} W/cm^2. Figure 5b shows the evolution of the

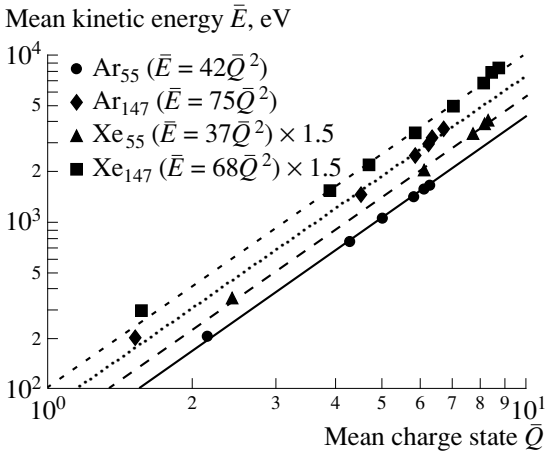

Fig. 4. Relation between the mean ion energy $\bar{E}$ and charge state $\bar{Q}$ obtained using different intensities (starting from the lowest value of $\bar{Q}$, 0.35, 1.4, 3.2, 5.6, 8.8, 13×10^{15} W/cm^2 for Ar_{55}, Ar_{147}, and Xe_{55}, and 0.35, 0.79, 1.0, 1.4, 1.9, 3.2, 13, 5.6, 8.8×10^{15} W/cm^2 for Xe_{147}). The values of $\bar{E}$ for Xe clusters were multiplied by 1.5 for clarity.

mean kinetic energy of ions from each subshell. From these figures we can see that electrons quit the cluster before the main stage of ion acceleration without exchanging significant energy with ions. This excludes a hydrodynamic scenario and indicates that the ions are accelerated mainly by their mutual Coulomb repulsion. Figure 5b also shows a stepwise character of the cluster explosion. The explosion is neither instantaneous nor uniform: the ions are accelerated in sequence from outer shells, and those leaving first are more energetic than those leaving later. This feature, also observed in one-dimensional Thomas-Fermi simulations [25] and in smoothed particle hydrodynamics simulations [26], can be understood on the basis of the ionization ignition mechanism [9] and Coulomb explosion. Seen by an ion in outer shells, the fields from the other ions add up to a large value while seen by an ion in inner shells, they cancel each other partly. Thus the ions in outer shells are ionized earlier and, at the same time, more effectively accelerated than those in inner shells.

Let us now turn to the charge-energy relation of individual ions. Rare gas clusters have a shell structure as is shown in the table. We consider the charge and energy distribution of ions originating from each subshell. We denote the mean kinetic energy of the ions with a charge of Q, originating from subshell s as $E_s(Q)$. It should be noted that neither $E_s(Q)$ nor its average over all the cluster subshells is identical to $\bar{E}$, plotted in Fig. 4. The latter is the mean energy of all the cluster ions, regardless of their charge state Q. On the other hand, for a given value of Q, $E_s(Q)$ involves only the

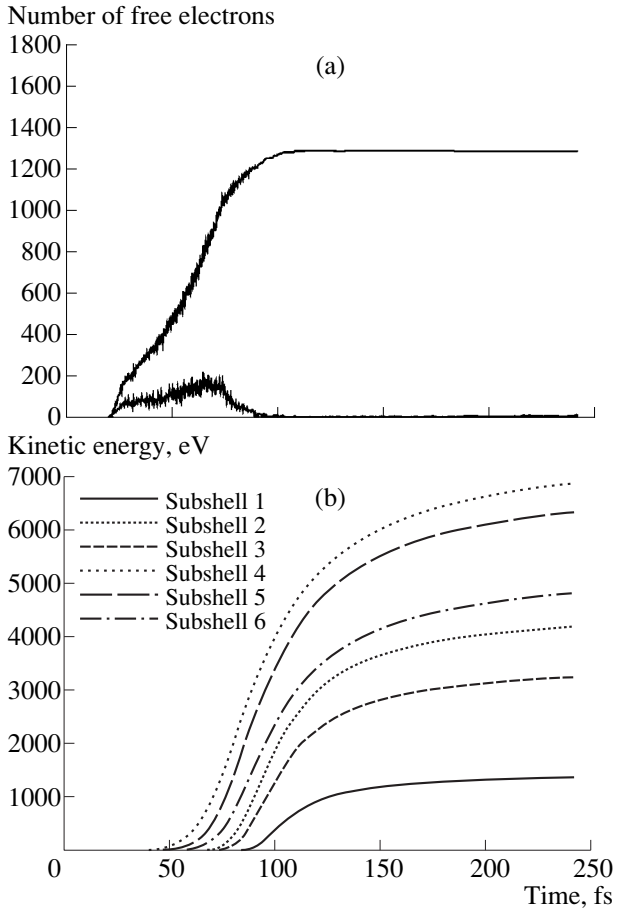

Fig. 5. (a) Evolution of the total number of free electrons (upper line) and the number of free electrons whose distance from the origin (the initial position of the central atom) is smaller than that of the outermost ion (lower line) for the case of a Xe_{147} cluster irradiated by the pulse with a peak intensity of 8.8×10^{15} W/cm^2. (b) Evolution of the mean ion energy of each subshell, for the case of (a).

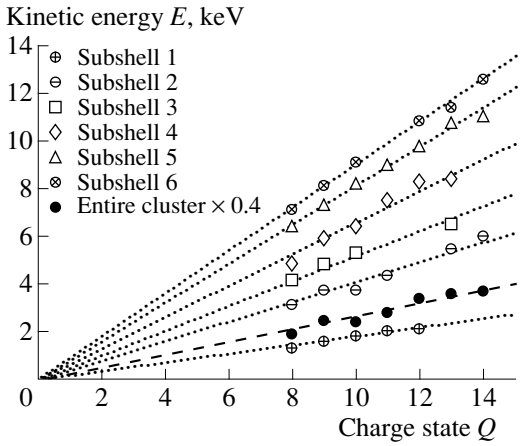

Fig. 6. Mean ion kinetic energy $E(Q)$ as a function of charge state Q for each subshell of Xe_{147} and for the entire cluster (filled circles, multiplied by 0.4 for clarity), in the case of a peak intensity 8.8×10^{15} W/cm^2. The subshells are enumerated outwards starting from the innermost one.

ions with this charge state. $\bar{E}$ can be written in terms of $E_s(Q)$ as,

$$\bar{E} = \frac{1}{N}\sum_s N_s \sum_Q Y_s(Q) E_s(Q), \tag{11}$$

where N_s is the number of the ions contained in subshell s, satisfying $N = \sum_s N_s$, while $Y_s(Q)$ is the probability distribution of Q in subshell s, normalized as $\sum_Q Y_s(Q) = 1$. Using $Y_s(Q)$, the mean charge state $\bar{Q}$ can be written as,

$$\bar{Q} = \frac{1}{N}\sum_s N_s \sum_Q Y_s(Q) Q. \tag{12}$$

In Fig. 6 we plot $E_s(Q)$ as a function of charge state Q for each subshell s (s = 1, …, 6) of Xe_{147} in the case of a peak intensity 8.8×10^{15} W/cm^2. We can model the relation in Fig. 6 with $E_s(Q) \approx \beta_s Q$, where a constant β_s depends on s. It should be emphasized that the approximately linear dependence in Fig. 6 is a consequence of the Coulomb explosion, which dominates the cluster explosion in our simulation results. This behavior can be understood as follows. Let us consider a pure Coulomb explosion of clusters composed of N ions with charges Q_i (i = 1, …, N) randomly chosen according to the probability distribution $Y_s(Q_i)$ depending on s. In general, the final kinetic energy E_1 of an ion with a charge Q_1 in subshell s_1 is a complicated function of $Q_1, \ldots, Q_N$. In order to estimate the average $\hat{E}_1$ of E_1 over the distribution of $Q_2, \ldots, Q_N$, we may assume that the cluster expands in average nearly isotropically and that the effect of the other ions in subshell s_1 is negligible. Then $\hat{E}_1$ can be roughly written as

$$\hat{E}_1(Q_1) \approx \frac{Q_1 \sum_{i \in s < s_1} \bar{Q}_i}{r_1} \propto Q_1, \tag{13}$$

where the sum is taken over all the ions in inner subshells and at the center, r_1 denotes the initial distance of the ion from the central ion, and $\bar{Q}_i \equiv \sum_{Q_i} Y_s(Q_i) Q_i$ is the expectation value of Q_i. The value of β_s is different from $\sum_{i \in s < s_1} \bar{Q}_i / r_1$ in general, since in simulations Q_i depends on time, there is screening of ion charges by free electrons, and the effect of the others ions in the same subshell is not completely negligible.

We simulated the Coulomb explosion of Xe_{147}, by dropping the electronic field term in the ionic equations of motion but taking account of the ion charge history obtained for the case of Fig. 6. The resulting charge-energy relation, shown in Fig. 7, is virtually the same as

that in Fig. 6. This confirms that the contribution of the electronic field to the acceleration of the ions is very small and that the linear relation is due to Coulomb explosion. If $Y_s(Q)$ is independent of s, the average $E(Q)$ of $E_s(Q)$ over the entire cluster is also proportional to Q. In Fig. 6 we have plotted $E(Q)$ as filled circles. We see a linear relation except for small deviation due to the dependence of $Y_s(Q)$ on s. We have found that this holds approximately also for Ar_{55}, Ar_{147}, and Xe_{55} and for other values of laser intensity. The preceding discussion has an important impact on the interpretation of the experimental results by Lezius *et al.* [2]. These authors attributed the linear dependence at higher charge states observed in their experiments to hydrodynamic expansion. Our results, however, indicate that this interpretation is not necessarily correct.

As we have already mentioned, Lezius *et al.* [2] found a quadratic charge dependence of ion energy for lower charge states and a linear dependence for higher charge states. We observe such a behavior in our simulation results (see below). In order to understand it, we have to take into account that the laser intensity has a spatial profile in experimental situations. Let us denote the mean energy and the relative yield of ions with a charge Q from clusters irradiated by a laser pulse with a peak intensity I by $E(I, Q)$ and $Y(I, Q)$, respectively. As we have seen in Fig. 6, $E(I, Q)$ can be roughly modeled with

$$E(I, Q) = \beta(I)Q, \tag{14}$$

where $\beta(I)$ is a coefficient depending on I. On the other hand, we can model the relation between

$$\bar{E}(I) \equiv \sum_Q Y(I, Q)E(I, Q), \tag{15}$$

and

$$\bar{Q}(I) \equiv \sum_Q Y(I, Q)Q, \tag{16}$$

with

$$\bar{E}(I) = \alpha\bar{Q}(I)^2, \tag{17}$$

as we have seen in Fig. 4. It follows from Eqs. (14) and (17) along with Eqs. (15) and (16) that

$$\beta(I) = \alpha\bar{Q}(I). \tag{18}$$

We can write the average $\langle E\rangle(Q)$ of $E(I, Q)$ over the spatial intensity profile, which corresponds to the charge-energy relation observed in experiments, as

$$\langle E\rangle(Q) = \frac{\alpha Q\int w(I)Y(I, Q)\bar{Q}(I)dI}{\int w(I)Y(I, Q)dI}, \tag{19}$$

where we have used Eqs. (14) and (18), and $w(I)$ is a weighting function, determined by the laser profile.

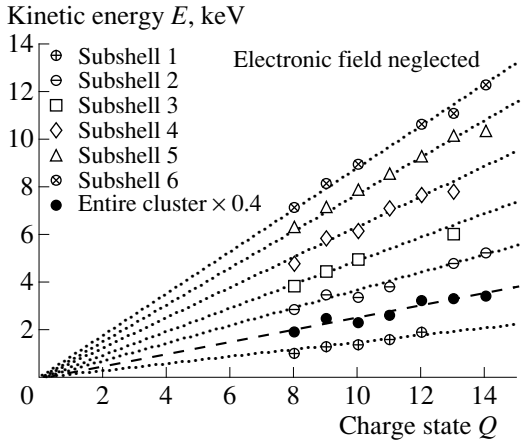

Fig. 7. Mean ion kinetic energy $E(Q)$ as a function of charge state Q for each subshell of Xe_{147} and for the entire cluster (filled circles, multiplied by 0.4 for clarity), obtained by neglecting the electronic field term in the-ionic equation of motion for the case of Fig. 6.

The mean charge state $\bar{Q}(I)$ is a function of intensity I and, in general, it takes a maximum at $I = I_{max}$, where I_{max} is the maximum peak intensity. It should be noted that $\bar{Q}(I_{max})$ is the maximum value of the mean charge state, *not* the highest charge state obtained. In fact, some ions have a charge much greater than $\bar{Q}(I_{max})$. We can divide the whole range of Q into two parts: $Q < \bar{Q}(I_{max})$ and $Q > \bar{Q}(I_{max})$.

In case where $Q < \bar{Q}(I_{max})$, the main contribution comes from such an intensity range that satisfies $\bar{Q}(I) \approx Q$, since $Y(I, Q)$ peaks at the value of Q around $\bar{Q}(I)$. Hence we may replace $\bar{Q}(I)$ in Eq. (19) by Q and obtain,

$$\langle E\rangle(Q) \approx \alpha Q^2 \propto Q^2 \quad \text{if} \quad Q < \bar{Q}(I_{max}). \tag{20}$$

On the other hand, for all the values of Q which satisfy $Q > \bar{Q}(I_{max})$, the most important contribution comes from the same spatial region of such high intensity that $\bar{Q}(I) \approx \bar{Q}(I_{max})$, since a significant portion of atoms are ionized to high charge states only there. Then, replacing $\bar{Q}(I)$ in Eq. (19) by $\bar{Q}(I_{max})$, we obtain,

$$\langle E\rangle(Q) \approx \beta(I_{max})Q \propto Q \quad \text{if} \quad Q > \bar{Q}(I_{max}). \tag{21}$$

In short, the behavior for $Q < \bar{Q}(I_{max})$, which reflects Eq. (17), contains the contribution from the entire intensity range, while that for $Q > \bar{Q}(I_{max})$ contains the contribution only from the intensity range close to I_{max}.

Figure 8 illustrates the ion energy-charge relation we obtained by taking average over the simulation results for Ar_{55}, Ar_{147}, Xe_{55}, and Xe_{147} with different

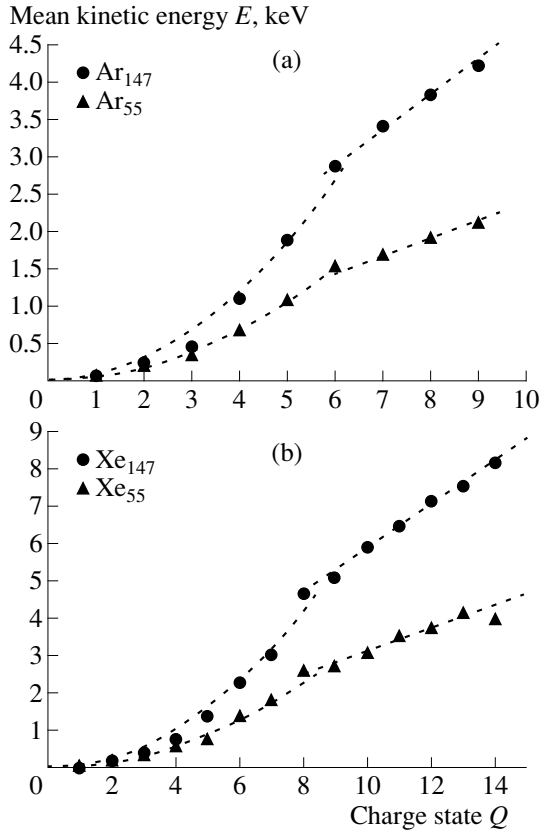

Fig. 8. Charge dependence of ion energy of (a) Ar_{55}, Ar_{147} and (b) Xe_{55}, Xe_{147} irradiated by the laser pulse with a peak intensity of 1.3×10^{16} W/cm^2, with account of the spatial intensity profile.

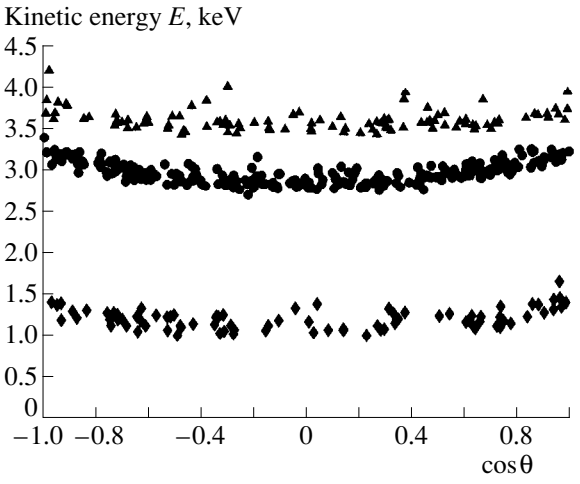

Fig. 9. Dependence of the kinetic energy on the cosine of the angle θ between the laser polarization vector and the emitted direction of the ions with a charge state of 8+ for the case of Xe_{55} irradiated by the laser pulse with a peak intensity of 1.3×10^{16} W/cm^2. Diamonds, circles, and triangles correspond to the ions originating from subshell 1, 2, and 3, respectively.

values of intensity as in Fig. 4. The average was taken with an equal weight, since our discussion in the previous paragraph does not depend much on the form of $w(I)$. As expected, for each of the four cases the dependence of ion energy $\langle E \rangle$ on Q is approximately quadratic for lower charge states $Q \le Q_c$ ($Q_c = 6$ for Ar, 8 for Xe) and linear for higher charge states $Q \ge Q_c$. These values of Q_c agree well with those of $\bar{Q}(I_{max})$, i.e., the highest value of the mean charge state that we can obtain from Fig. 4. It should be emphasized again that the charge-energy relation in Fig. 8 is a consequence of Coulomb explosion.

In [2] the relation was reported to be quadratic in the entire range of $1 \le Q \le 8$ in the case of Ar. This may be explained as follows. The laser intensity needed to obtain Ar^{8+} and Ar^{9+} via tunnel ionization is 2.6×10^{16} W/cm^2 and 1.6×10^{18} W/cm^2, respectively. The large difference between these two values is due to the fact that the ionization potential of Ar^{8+} (422 eV [27]) is much higher than that of Ar^{7+} (143 eV [27]). The peak intensity (5×10^{17} W/cm^2) used in [2] was sufficient to obtain a significant number of Ar^{8+}, but too low to ionize Ar nine times even with the aid of the ionization ignition mechanism. Since this corresponds to $\bar{Q}(I_{max}) = 8$, a quadratic charge-energy relation was observed for $1 \le Q \le 8$. On the other hand, the yield of Ar^{Q+} ($Q \ge 9$), for which a linear dependence should be expected, was very low.

5. CONCLUSIONS

We have studied the ionization and explosion of rare gas clusters in an intense laser field using Monte Carlo particle dynamics simulations. The ionization ignition mechanism [9] dominates ionization of cluster atoms, while the electron impact ionization plays only a minor role. This follows from the fact that the electron mean free path with respect to this process is typically larger than the cluster size. Our results show that cluster ions are accelerated in sequence from outer shells by the Coulomb repulsion force between themselves. Free electrons escape from the cluster without exchanging significant energy with ions, and hardly contribute to the cluster explosion. The entire charge dependence of ion kinetic energy, including a linear part at higher charge states, formerly attributed to hydrodynamic expansion, can be understood as a consequence of Coulomb explosion and the effect of the spatial laser intensity variation. Our finding can affect the interpretation of experimental results.

It is true that our simulation results cannot directly exclude the possibility of hydrodynamic expansion in larger clusters containing over 1000 atoms. However, it is striking that the overall feature of the charge-energy relation in Fig. 8 is similar to the one obtained in the experiments by Lezius *et al.* [2]. Last and Jortner [10, 11] showed that electrons quickly leave even large

clusters containing 2097 atoms. Moreover, according to our results, the energy of ions is slightly higher when they are emitted along the direction of laser polarization than perpendicular to it (see Fig. 9), which agrees with a recent experimental finding [28]. These agreements strongly indicate that the cluster explosion may be essentially governed by Coulomb explosion even in such large clusters.

REFERENCES

1. Lezius, M., Dobosz, S., Normand, D., and Schmidt, M., 1997, *J. Phys. B*, **30**, L251.
2. Lezius, M., Dobosz, S., Normand, D., and Schmidt, M., 1998, *Phys. Rev. Lett.*, **80**, 261.
3. Ditmire, T., Tisch, J.W.G., Springate, E., *et al.*, 1997, *Nature* (London), **386**, 54.
4. Shao, Y.L., Ditmire, T., Tisch, J.W.G., *et al.*, 1996, *Phys. Rev. Lett.*, **77**, 3343.
5. Thompson, B.D., McPherson, A., Boyer, K., and Rhodes, C.K., 1994, *J. Phys. B*, **27**, 4391.
6. Boyer, K., Thompson, B.D., McPherson, A., and Rhodes, C.K., 1994, *J. Phys. B*, **27**, 4373.
7. Ditmire, T., Donnelly, T., Rubenchik, A.M., *et al.*, 1996, *Phys. Rev. A*, **53**, 3379.
8. Ditmire, T., 1998, *Phys. Rev. A*, **57**, R4094.
9. Rose-Petruck, C., Schafer, K.J., Wilson, K.R., and Barty, C.P.J., 1997, *Phys. Rev. A*, **55**, 1182.
10. Last, I. and Jortner, J., 1998, *J. Phys. Chem. A*, **102**, 9655.
11. Last, I. and Jortner, J., 1999, *Phys. Rev. A*, **60**, 2215.
12. Corkum, P.B., Burnett, N.H., and Brunel, F., 1989, *Phys. Rev. Lett.*, **62**, 1259.
13. Corkum, P.B., 1993, *Phys. Rev. Lett.*, **71**, 1994.
14. Clementi, E. and Raimondi, D.L., 1963, *J. Chem. Phys.*, **38**, 2686.
15. Press, W.H., Teukolsky, S.A., Vetterling, W.T., and Flannery, B.P., 1992, *Numerical Recipes in FORTRAN* (Cambridge: Cambridge Univ. Press).
16. Kustaanheimo, P. and Stiefel, E., 1965, *J. Reine Angew. Math.*, **218**, 204.
17. Aarseth, S.J., 1985, in *Multiple Time Scales*, Brackbill, J.U. and Cohen, B.I., Eds. (Orlando: Academic), p. 377.
18. Brumberg, V.A., 1995, *Analytical Technigues of Celestial Mechanics* (Berlin: Springer-Verlag).
19. Perelomov, A.M., Popov, V.S., and Terent'ev, M.V., 1966, *Sov. Phys. JETP*, **23**, 924.
20. Ammosov, M.V., Delone, N.B., and Krainov, V.P., 1986, *Sov. Phys. JETP*, **64**, 1191.
21. Lennon, M.A., Bell, K.L., Gilbody, H.B., *et al.*, 1988, *J. Phys. Chem. Ref. Data*, **17**, 1285.
22. Lotz, W., 1968, *Z. Phys.*, **216**, 241.
23. Northby, J.A., 1987, *J. Chem. Phys.*, **87**, 6166.
24. Bondi, A., 1964, *J. Phys. Chem.*, **68**, 441.
25. Brewczyk, M. and Rzążewski, K., 1999, *Phys. Rev. A*, **60**, 2285.
26. Rusek, M., Lagadec, H., and Blenski, T., unpublished.
27. Cowan, R.D., 1981, *The Theory of Atomic Structure and Spectra* (Berkeley: Univ. of California Press), p. 12.
28. Springate, E., Hay, N., Tisch, J.W.G., *et al.*, 2000, *Phys. Rev. A*, **61**, 063201.